genesis 49:862–869 (2011)

TECHNOLOGY REPORT

Generation of Mice With a Conditional Allele for the p75^{NTR} Neurotrophin Receptor Gene

Emil Bogenmann,[1]* Penny S. Thomas,[2] Qianfeng Li,[2] Jieun Kim,[3] Liang-Tung Yang,[3] Brian Pierchala,[2] and Vesa Kaartinen[2,3]*

[1]Department of Pediatrics, The Saban Research Institute of Children's Hospital Los Angeles, Los Angeles, California

[2]Department of Biologic and Materials Sciences, University of Michigan, Ann Arbor, Michigan

[3]Department of Pathology, The Saban Research Institute of Children's Hospital Los Angeles, Los Angeles, California

Received 1 December 2010; Revised 1 March 2011; Accepted 7 March 2011

Summary: The p75^{NTR} neurotrophin receptor has been implicated in multiple biological and pathological processes. While significant advances have recently been made in understanding the physiologic role of p75^{NTR}, many details and aspects remain to be determined. This is in part because the two existing knockout mouse models (Exons 3 or 4 deleted, respectively), both display features that defy definitive conclusions. Here we describe the generation of mice that carry a conditional p75^{NTR} (p75$^{NTR\text{-}FX}$) allele made by flanking Exons 4–6, which encode the transmembrane and all cytoplasmic domains, by loxP sites. To validate this novel conditional allele, both neural crest-specific p75^{NTR}/Wnt1-Cre mutants and conventional p75^{NTR} null mutants were generated. Both mutants displayed abnormal hind limb reflexes, implying that loss of p75^{NTR} in neural crest-derived cells causes a peripheral neuropathy similar to that seen in conventional p75^{NTR} mutants. This novel conditional p75^{NTR} allele will offer new opportunities to investigate the role of p75^{NTR} in specific tissues and cells. genesis 49:862–869, 2011. **© 2011 Wiley Periodicals, Inc.**

Key words: nerve growth factor receptor; signaling; mouse mutant; growth retardation; nerve abnormalities

The p75 neurotrophin receptor (p75^{NTR}) is a transmembrane protein composed of an extracellular domain containing several cysteine-rich motifs, a transmembrane domain, and a non-catalytic intra-cellular domain (Underwood and Coulson, 2008). It can interact with multiple different ligands and co-receptors and has been implicated in the regulation of a myriad cellular process including survival, neurite outgrowth and myelinization (Roux and Barker, 2002). p75^{NTR} can bind all four neurotrophins and can also enhance signal transduction by Trk tyrosine kinase receptors in response to neurotrophins via a mechanism that is not fully understood (Underwood and Coulson, 2008). Moreover, p75^{NTR} can form a molecular complex with the Nogo receptor and transduce myelin inhibitory signals, and associate with ephrin-A receptors and communicate reverse EphA signaling (Barker, 2004; Lim *et al.*, 2008). Some of the functions of p75^{NTR} likely involve the proteolytic cleavage of its extracellular domain by metalloproteases followed by cleavage of the transmembrane domain by γ-secretase (Bronfman, 2007). This results in the production of an intracellular fragment that translocates to the nucleus and participates in transcriptional events.

To address the role of p75^{NTR} in vivo, Lee *et al.* generated a knockout mouse by deleting Exon 3, which encodes part of the extracellular domain (Lee *et al.*, 1992). Homozygote mice are viable and fertile, and do not show any obvious external phenotypes. However, they display several defects in the nervous system, such

Current address for Liang-Tung Yang: Institute of Cellular and System Medicine, National Health Research Institutes, Miaoli County, Taiwan, ROC.

*Correspondence to: Vesa Kaartinen, Biologic and Materials Sciences, University of Michigan, Ann Arbor, MI. E-mail: vesak@umich.edu or Emil Bogenmann, Pediatrics, The Saban Research Institute of Children's Hospital Los Angeles, Los Angeles, CA. E-mail: ebogenmann@chla.usc.edu

Contract grant sponsor: NIH; Contract grant numbers: HL074862, DE013085.

Published online 16 March 2011 in
Wiley Online Library (wileyonlinelibrary.com).
DOI: 10.1002/dvg.20747

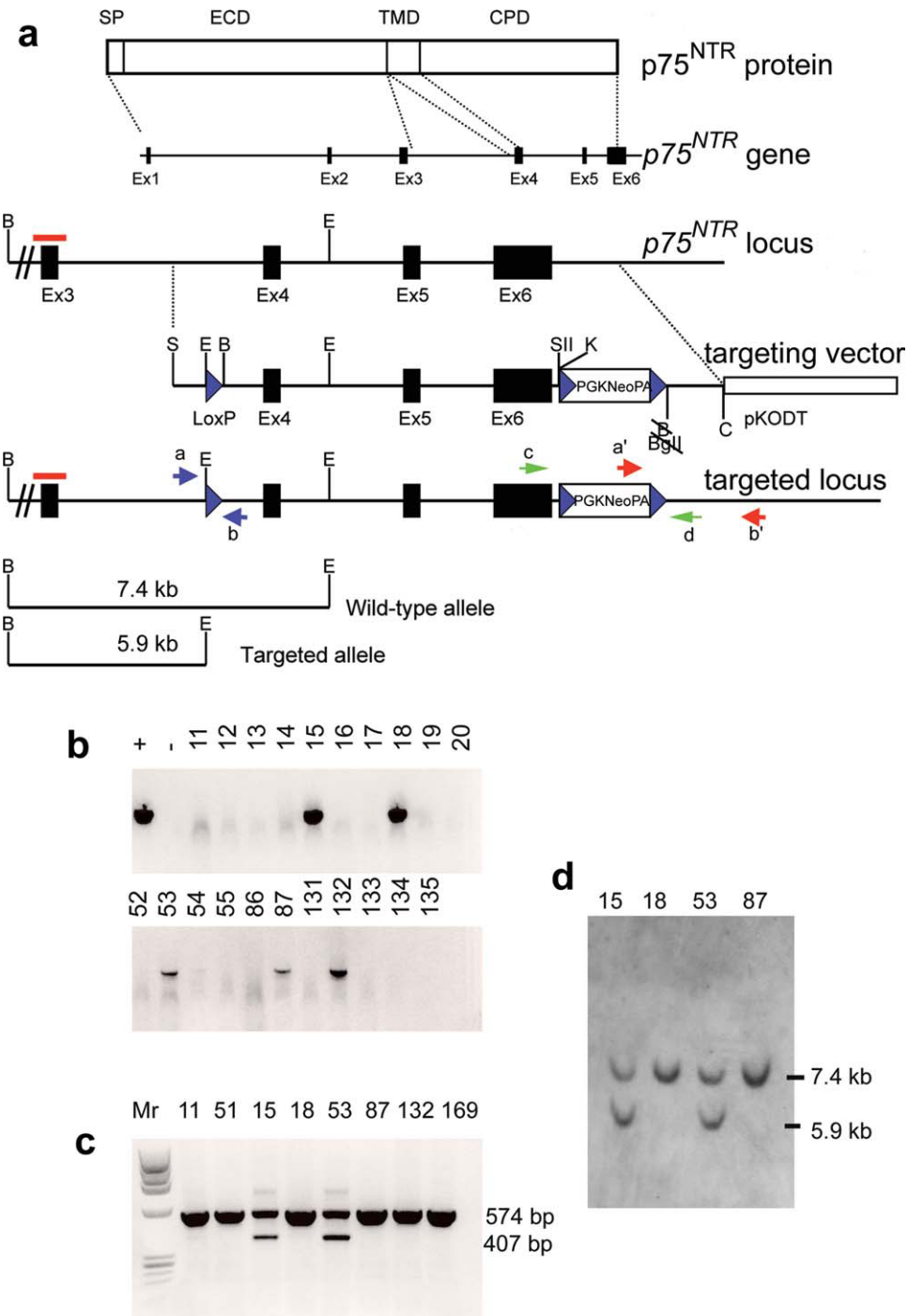

FIG. 1. *p75^{NTR}* targeting vector and screening of ES colonies. (**a**) A schematic presentation of p75^{NTR} protein domains; the *p75^{NTR}* genomic locus depicting a segment from Exon 3 to Intron 6; the *p75^{NTR}* targeting vector and the *p75^{NTR}* targeted allele. (**b**) An example of a PCR screen using primers a′ and b′ (red arrows) to identify correctly targeted ES cell clones; positive clones: #15, #18, #53, #87, and #132; "+" and "−" depict the positive and negative controls, respectively [(a′) = 5′-GGGGATCCGCTGTAAGTCTGCA-3′ and (b′) 5′-TGGGGGAGGGGTGGCTAATTT-3′). (**c**) PCR analysis using a/b primers (blue arrows in a; (a) 5′-CCTCCGCCAGCTGTCTGCTTCCT-3′ and a reverse primer (b) 5′-GGGTGGAAGCTGGGACTGTGCACATGC-3′) and template DNA from the putative correctly targeted clones (b) demonstrate that the clones #15 and #53 had retained the 5′ *loxP* site. The wild type allele produces a 574-bp amplification product. Since the strategy to insert the 5′ *loxP* sites into Intron 3 involved the generation of a 207-bp deletion, the mutant allele gives rise to a 407-bp amplification product. (**d**) Verification of the correct targeting using Southern blot analysis. Genomic ES cell DNAs were digested with *Bam*HI and *Eco*RI and probed with the external probe (red bar in a). Correctly targeted clones #15 and #53 display both the wild-type and targeted alleles of 7.4 and 5.9 kb, respectively, while the non-targeted clones #18 and #87 show only the wild-type allele (7.4 kb). [Color figure can be viewed in the online issue, which is available at wileyonlinelibrary.com.]

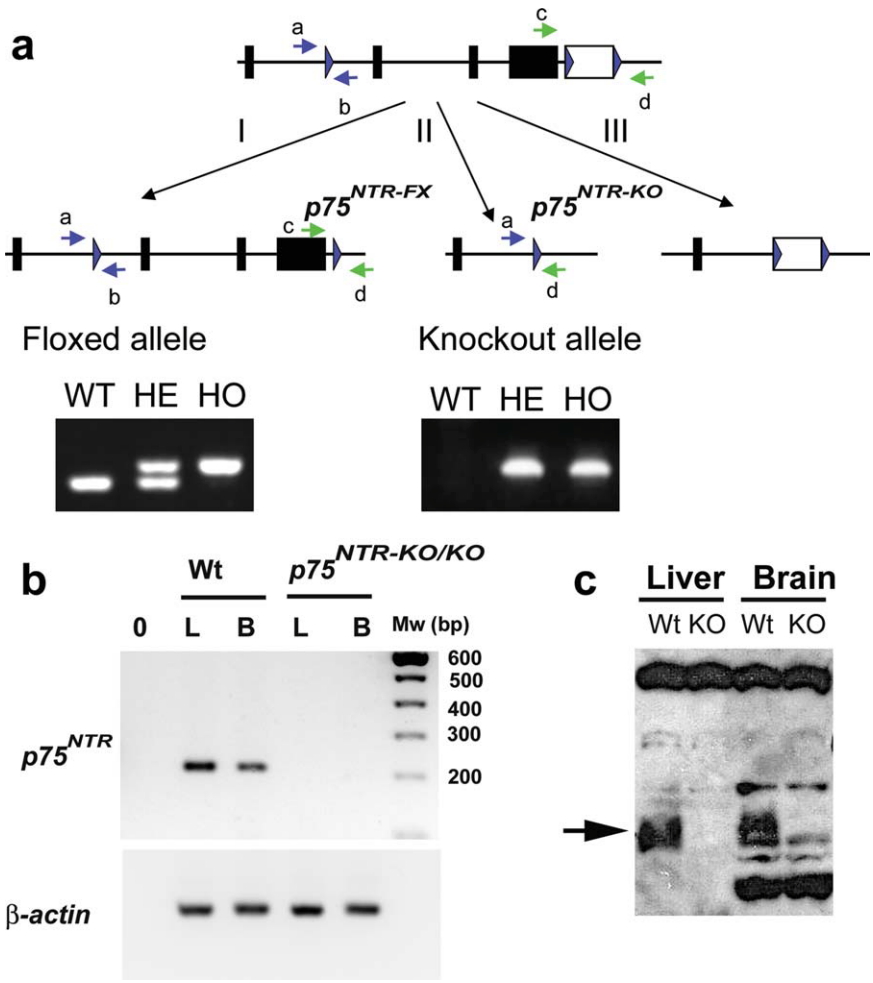

FIG. 2. Generation of mice carrying the floxed ($p75^{NTR\text{-}FX}$) and knockout ($p75^{NTR\text{-}KO}$) *p75* alleles. (**a**) Transgenic *Ella-Cre* mice were crossed with mice homozygous for the *p75* targeting vector. The resulting mosaic males were further crossed with wild-type females to obtain $p75^{NTR\text{-}FX/WT}$ mice (Type I recombination; green arrows c and d depict the primers used [(c) 5′-TGCAGAAATCATCGACCCTTCCC-3′ and (d) 5′-TCCTCACCCCGTTCTTTCCCC-3′]; upper panel) and $p75^{NTR\text{-}KO/WT}$ mice (Type II recombination; blue and green arrows depict the forward and reverse primers, respectively; upper panel). Tail DNAs were analyzed using PCR to identify samples carrying the floxed allele (lower left panel; primers shown with blue arrows in the upper panel) or the knockout allele (lower right panel; primers shown with blue (forward) and green (reverse) arrows in the upper panel). WT, wild type; HE, heterozygote; HO homozygote. (**b**) RT-PCR analysis of RNAs isolated from brain (B) or liver (L) tissues of 8-week-old control and *p75* knockout mice demonstrates that *p75* knockout tissues did not contain any detectable *p75* mRNA (upper panel), while control samples showed the expected 210-bp amplification product. β-actin-specific primers produced a 245-bp amplification product of comparable intensity in all samples (bottom panel). (**c**) Western blot analysis of protein lysates shows that $p75^{NTR}$ protein is present in wild-type (Wt) brain and liver tissues, while knockout (KO) tissues do not display any detectable protein (arrow points to the $p75^{NTR}$ protein band). [Color figure can be viewed in the online issue, which is available at wileyonlinelibrary.com.]

as impaired innervation by peripheral sensory neurons and decreased sensitivity to NGF (Lee *et al.*, 1994a,b). Subsequently, von Schack *et al.* showed that $p75^{NTR\Delta Exon3}$ encodes an alternatively spliced isoform, which is apparently present both in wildtype and in homozygote $p75^{NTR\Delta Exon3}$ mice (von Schack *et al.*, 2001). Reasoning that this isoform was able to support some signaling activity, these investigators generated another p75 mouse line that lacks sequences encoded by Exon 4 ($p75^{NTR\Delta Exon4}$) (von Schack *et al.*, 2001). The $p75^{NTR\Delta Exon4}$ mice display more severe defects than $p75^{NTR\Delta Exon3}$ mutants: about 40% of them die during the late fetal or early postnatal period, and showed defects in the descending aorta. The surviving mice are growth-retarded during the first weeks of life, and have abnormal reflexes and impaired motility caused by hind limb ataxia. It was later shown that the $p75^{NTR\Delta Exon4}$ mutants express an intracellular fragment of $p75^{NTR}$ that has pro-apoptotic properties (Paul *et al.*, 2004). In summary, two different mutant mouse strains deficient in $p75^{NTR}$ have been developed which illuminated new functions of the receptor in vivo (Lee *et al.*, 1992; von Schack *et al.*, 2001). Unfortunately, interpretation of the phenotypes of these mutant strains is complicated by

novel and unanticipated molecular signals. Thus, additional mutant mouse strains are required to clarify the debate about the various functions of *p75^{NTR}*.

We generated such a novel mouse line carrying a conditional knockout allele for *p75^{NTR}* (*p75$^{NTR\text{-}FX/FX}$*) to investigate its functions in specific cells and tissues *in vivo*. The allele was designed such that a complete and conditional knockout can be achieved without the molecular complexities observed in mice with either the *p75$^{NTR\Delta Exon3}$* (von Schack *et al.*, 2001) or the *p75$^{NTR\Delta Exon4}$ allele* (Paul *et al.*, 2004). Our strategy was to flank Exons 4–6, which encodes the transmembrane and cytoplasmic domains, by *loxP* sites. The short (1.6 kb) and long (8.6 kb) arms of the targeting vector were PCR amplified from a Bac genomic DNA. A single *loxP* site was inserted into Intron 3 and the *loxPNeoloxP* cassette was inserted into the 3′ sequence following the last Exon 6 (see Fig. 1). As a negative selection marker we used the *diphteria toxin (DT)* gene. The linearized targeting vector was electroporated into *TVB2* embryonic stem cells as described (Yang and Kaartinen, 2007). Five out of 150 G418-resistant colonies showed locus-specific integration (Fig. 1b). Subsequent PCR and Southern assays confirmed that 2 of them contained the distant 5′ *loxP* site (Fig. 1c,d). Both correctly targeted ES clones were able to produce highly chimeric male mice, which were potent germline transmitters. To remove the *Neo* selection marker and to generate a presumed knockout allele for *p75^{NTR}*, we crossed the *p75$^{NTR\text{-}FXNeo/FXNeo}$* mice (homozygotes for the targeting vector) with *EIIa-Cre* transgenic mice (Holzenberger *et al.*, 2000; Xu *et al.*, 2001). The obtained mosaic male progeny were subsequently crossed with wild-type female mice to obtain floxed (*p75$^{NTR\text{-}FX}$*) and null (*p75$^{NTR\text{-}KO}$*) allele-carrying mouse lines (Fig. 2a). Homozygote *p75$^{NTR\text{-}FX/FX}$* mice were viable and fertile, and did not display any overt phenotypes.

To confirm that the *p75$^{NTR\text{-}KO}$* allele encoded a true null allele and to provide initial information about the biological role of *p75^{NTR}*, we inter-crossed the heterozygote *p75$^{NTR\text{-}KO/WT}$* mice to obtain homozygote *p75$^{NTR\text{-}KO/KO}$* mice. Genotype analyses of newborn offspring showed the expected Mendelian ratio of wild-type (*p75$^{NTR\text{-}WT/WT}$*), heterozygotes (*p75$^{NTR\text{-}KO/WT}$*), and homozygotes (*p75$^{NTR\text{-}KO/KO}$*) consistent with viability of the *p75$^{NTR\text{-}KO/KO}$* at birth ($n = 63$). RT-PCR using primers with target sequences in Exons 4 and 6 of brain and liver samples confirmed that the knockout allele did not produce any detectable amplification product, while the wild-type control showed the expected 210-bp fragment (Fig. 2b). Immunoblotting using an antibody which recognizes the cytoplasmic domain of p75^{NTR} confirmed the absence of a *p75^{NTR}* gene product in *p75$^{NTR\text{-}KO/KO}$* mice (Fig. 2c). Homozygote *p75$^{NTR\text{-}KO/KO}$* mice showed notable growth retardation during the first weeks of life, but subsequently recovered so that by the age of 10 weeks the size difference between *p75^{NTR}* mutants and controls was eliminated (Fig. 3a,b). Starting at about three weeks of age, *p75^{NTR}* null mutants displayed signs of neuropathic phenotypes. When suspended by the tail, they clenched their hind limbs under their body, while the controls displayed the normal behavior of spreading out their hind limbs and toes (Fig. 5a,b).

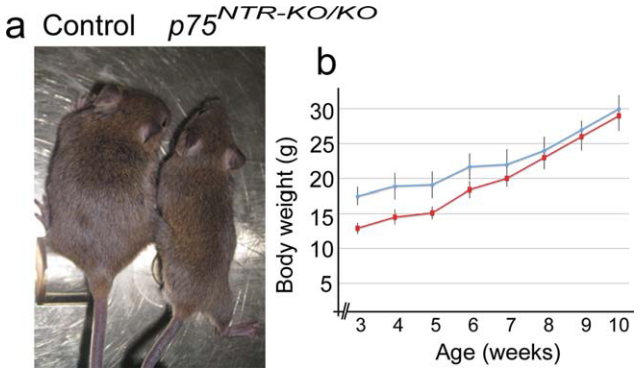

FIG. 3. p75$^{NTR\text{-}KO/KO}$ mice are smaller than their wild-type littermates. (**a**) A *p75$^{NTR\text{-}KO/KO}$* mouse is smaller (right) than its control littermate (left) at 4 weeks of age. (**b**) A line graph depicting the size difference between mutant (red line) and control (blue line) mice from 3 weeks of age to 12 weeks of age (three mice were used in each group).

Since *p75^{NTR}* is strongly expressed in migrating neural crest cells (NCCs), we generated tissue-specific *p75^{NTR}* mutants by crossing *p75$^{NTR\text{-}FX/FX}$* mice with transgenic *Wnt1-Cre* driver mice, which are known to be able to induce a robust recombination in early migratory NCCs (Chai *et al.*, 2000; Jiang *et al.*, 2000). Tissue-specific *p75^{NTR}/Wnt1-Cre* mutants were born in the expected Mendelian numbers and did not display subsequent growth retardation as observed in conventional *p75^{NTR}* mutants. Lack of p75 protein in the *Wnt1* recombination domain was confirmed by p75^{NTR} immunostaining. As shown in Figure 4, p75^{NTR} was specifically ablated in the dorsal root ganglia (derived from NCCs), while its expression in the lateral motor column was unaffected at E10. *p75^{NTR}/Wnt1-Cre* mutants displayed an abnormal hind limb "clenching" phenotype similar to that seen in conventional *p75^{NTR}* mutants suggesting that this common neuropathic phenotype was at least in part due to the impaired function of p75^{NTR} specifically in neural crest cells (Fig. 5c,d). Previous studies have shown that sciatic nerves are abnormal in both *p75$^{NTR\Delta Exon3}$* and *p75$^{NTR\Delta Exon4}$* mutants (von Schack *et al.*, 2001). Concordant with these findings, the sciatic nerves in *p75$^{NTR\text{-}KO/KO}$* mice showed about a 30% reduction in diameter when compared to those of control littermates (Fig. 5e–g). In addition, there were far fewer small diameter axon bundles in the mutant nerves than in control nerves suggesting that *p75^{NTR}*

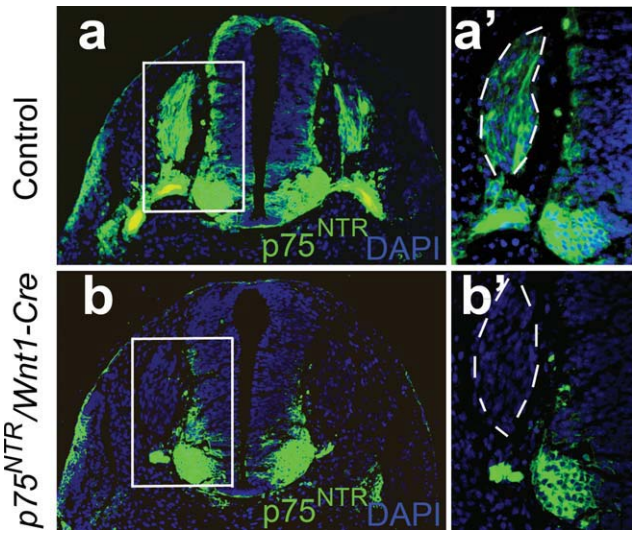

FIG. 4. p75^{NTR} protein is efficiently ablated from the dorsal root ganglia in *p75^{NTR}/Wnt1-Cre* mutants. (**a**) In controls p75^{NTR} can be detected both in the neural crest-derived dorsal root ganglia (DRG) and in the lateral motor column at E10. (**a′**) higher power view identifying the DRG (circled with the white hatched line). (**b**) In *p75^{NTR}/Wnt1-Cre* mutants, p75^{NTR} is present in the lateral motor column, but not in the DRG. (**b′**) shows the high power image of the region indicated in b. An area circled with the hatched line indicates the DRG region that does not stain positively for p75^{NTR} protein.

mutants may suffer from defects in nociceptive sensory inputs, which are mostly unmyelinated and lightly-myelinated small diameter axons (Fig. 5h,i).

Van Schack *et al.* have reported that the homozygous *p75$^{NTR\Delta Exon3}$* mutants are born with expected Mendelian frequency, but about 40% of corresponding *p75$^{NTR\Delta Exon4}$* mutant mice die during the perinatal period and suffer from pronounced vascular defects (von Schack *et al.*, 2001). Here we show that deletion of the transmembrane and the entire cytoplasmic domain from the *p75^{NTR}* gene does not lead to late gestational, perinatal, or neonatal lethality. Neither could we detect vasodilatation phenotype in the dorsal aorta comparable to that seen in *p75$^{NTR\Delta Exon4}$* mutants (data not shown). Instead our present studies demonstrate that at least some of the neurological phenotypes result from the need for functional p75^{NTR} in the neural crest cell lineage, while a role for p75^{NTR} in non-neural crest is implied by retardation in postnatal growth in systemic but not *Wnt1-Cre*-driven conditional mutants. Whether the more severe phenotype in *p75$^{NTR\Delta Exon4}$* mutants when compared either to *p75$^{NTR\Delta Exon3}$* mutants or to *p75$^{NTR/KOKO}$* mutants described in this article results from a production of an aberrant pro-apoptotic peptide as previously suggested (Paul *et al.*, 2004), from background differences or from other currently unknown reasons remains to be shown.

The mutant *p75$^{NTR/KO}$* allele described here does not produce a detectable protein product. Therefore, future studies using this allele will not be hampered by complexities associated with the use of the *p75$^{NTR\Delta Exon3}$* allele, which produces an alternatively spliced product (von Schack *et al.*, 2001), or with the use of the *p75$^{NTR\Delta Exon4}$* allele, which expresses an aberrantly pro-apoptotic peptide (Paul *et al.*, 2004). Similarly, the recently described p75^{NTR} conditional allele, in which Exon 3 was flanked by loxP sites (Lim *et al.*, 2008), can be expected to produce a similar alternative splicing variant as described for the corresponding conventional knockout allele (Lee *et al.*, 1992). However, Cre-mediated recombination of the *p75$^{NTR\text{-}FX}$* conditional allele described here leads to a complete inactivation of the *p75^{NTR}* gene. Recent studies have shown that expression levels of *p75^{NTR}* undergo dynamic changes during tissue injury and regeneration (Peterson and Bogenmann, 2003; Tomita *et al.*, 2007), but the detailed role of p75^{NTR} in these processes is currently unknown. The novel mouse line described here opens new opportunities to address tissue and cell type-specific roles of *p75^{NTR}* in physiologic and pathologic conditions.

METHODS

Generation of Mice Carrying the Floxed and Knockout *p75^{NTR}* Alleles

The long arm of the targeting vector containing the loxP site in Intron 3 was prepared as follows: A short (about 1.6 kb) *Sal*I-*Eco*RI 5′ fragment and a long (about 7 kb) *Bam*HI-*Sac*II 3′fragment were PCR amplified using RP23-67E18 Bac as a template. These fragments were subcloned and a single loxP site was inserted between the *Eco*RI and *Bam*HI sites. The large (about 8.7 kb) 5′ arm containing a loxP site in Exon 3 was then isolated as a single *Sal*I-*Sac*II fragment. The short, 3′, arm was amplified using RP23-67E18 Bac as a template as a single *Xho*I-*Cla*I fragment. High-fidelity Supermix (Qiagen) polymerase was used for amplification, and the generated arms were sequenced to verify that no PCR-generated mutations had been introduced. The targeting vector was assembled by first subcloning the *PGK-Neo* cassette flanked by loxP sites as a *Kpn*I-*Bgl*II fragment into pKODT digested with *Kpn*I-*Bam*HI. Next the long *Sal*I-*Sac*II fragment (the long arm) containing the loxP site in Intron 3 was added into loxP-*PGK-Neo-loxP/*pKODT and finally the short arm was added into the construct as a *Cla*I-*Xho*I fragment. The targeting vector was electroporated into TVB2 mouse ES cells, and recombinant ES cell clones were selected with *G418* as described (Dudas *et al.*, 2004; Kaartinen *et al.*, 1995). Mouse chimeras were generated by injecting correctly targeted ES clones into C57BL/6J mouse blastocysts. The floxed *p75^{NTR}* allele (*p75$^{NTR\text{-}FX}$*) and the knockout *p75^{NTR}* allele (*p75$^{NTR\text{-}KO}$*) were generated by crossing female mice homozygous for the targeting vec-

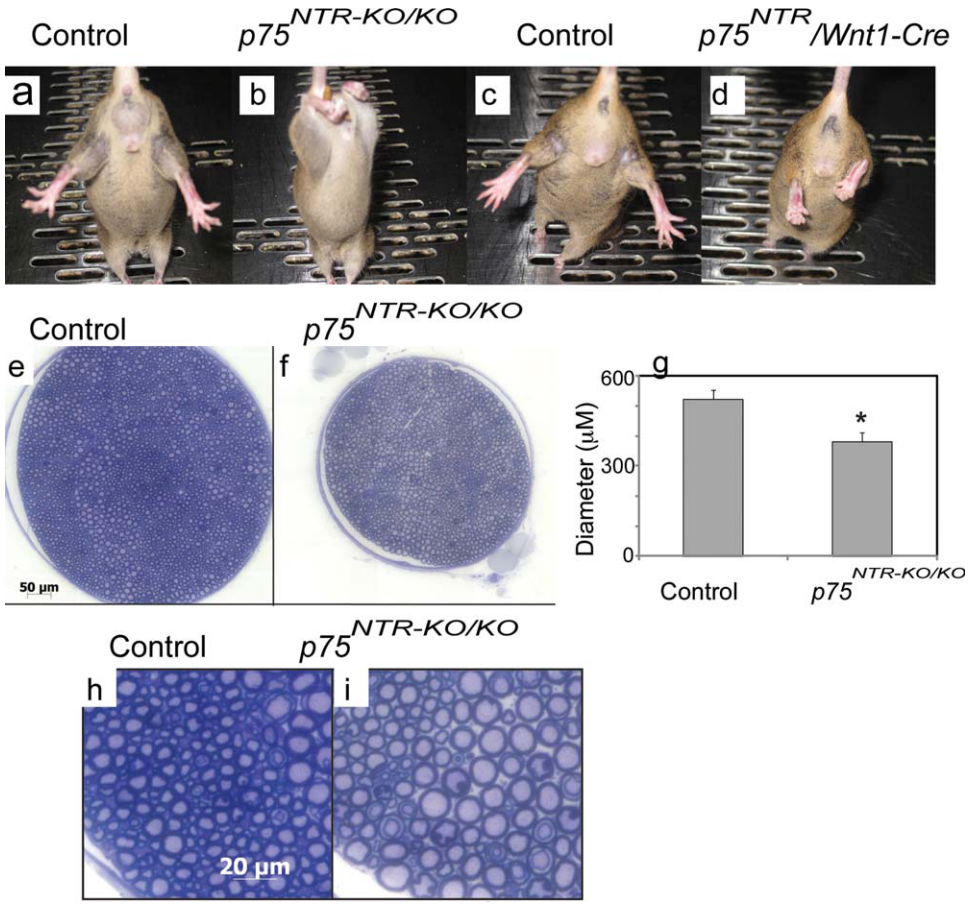

FIG. 5. Neurological defects in *p75^{NTR}* mutants. When suspended by the tail, both *p75$^{NTR-KO/KO}$* (**b**) and *p75^{NTR}/Wnt1-Cre* (**d**) mutants display an abnormal hind limb "clenching" response, while corresponding controls (**a** and **c**) show a normal "stretching" response. Sciatic nerves of adult (1- to 3-months old) *p75^{NTR}* mutants (**f**) show about a 30% reduction in diameter when compared to those of control littermates (**e**). (**g**) Bar chart showing quantitation of the difference in axon diameter between controls and *p75^{NTR}* mutants. (**i**) *p75^{NTR}* mutant sciatic nerves display a statistically significant lower number of small diameter unmyelinated and lightly-myelinated axons when compared to those of controls (**h**).

tor with *EIIa-Cre* transgenic male mice (Xu *et al.*, 2001). Both *EIIa-Cre* and *Wnt1-Cre* mice were from The Jackson Laboratories (Maine).

PCR Screening, Clone Verification, and Genotyping

ES cell DNAs were first screened for correct targeting by PCR using a forward primer (a′) 5′-GGGGATCCG CTGTAAGTCTGCA-3′ and a reverse primer (b′) 5′-TGGGGGAGGGGTGGCTAATTT-3′. Subsequently, presence of the single *loxP* site in Intron 4 was verified by PCR using a forward primer (a) 5′-CCTCCGCCAGCT GTCTGCTTCCT-3′ and a reverse primer (b) 5′-GGGTGG AAGCTGGGACTGTGCACATGC-3′. *p75^{NTR-FX}* mice were genotyped using forward and reverse primers (c) 5′-TGCAGAAATCATCGACCCTTCCC-3′ and (d) 5′-TCCTCA CCCCGTTCTTTCCCC-3′, respectively, while *p75^{NTR-KO}* mice were genotyped using forward (a) and reverse primers (d). Southern blot analyses of genomic DNAs digesting with *Bam*HI and *Eco*RI were used to confirm homologous recombination using an external probe, which recognizes sequences encoded by Exon 3 (see Fig. 1).

Timed Matings and Embryo Generation

Mice were maintained on a daily twelve hour light cycle and female mice checked for vaginal plugs twice a day. The day on which a female mouse acquired a vaginal plug was designated as day ("E") 0. For the required embryonic stages, pregnant females were euthanized by CO_2 after the appropriate number of days and embryos were recovered for analysis. All studies and procedures performed on mice were carried out at the Animal Care Facility of the School of Dentistry (ULAM), University of Michigan-Ann Arbor, and were approved by the University of Michigan Animal Care and Use Committee

(UCUCA). The mice were maintained in mixed genetic backgrounds.

RT-PCR

Total RNA was isolated from E8 embryos (RNeasy mini kit, Qiagen), and cDNAs synthesized (Omniscript reverse transcription kit, Qiagen) according to manufacturer's protocols. cDNAs were analyzed by PCR for $p75^{NTR}$ expression using the following primer pairs. β-actin was used as a quality and loading control.

$p75^{NTR}$-*S* 5′	GGCAGCTCCCAGCCTGTAGTGACC 3′
$p75^{NTR}$-*AS* 5′	CCGCTGTCGCTGTGCAGTTTC 3′
β-*actin-S* 5′	GTGGGCCGGTCTAGGCACCAA 3′
β-*actin-AS* 5′	CGGTTGCCTTAGGGTTCAGG 3′

Western Blotting

Brain and liver tissues were harvested from three week old control and mutant mice, and lysed in 2× Laemmli sample buffer (Harlow and Lane, 1988). About 10 μg of protein per lane was resolved on NuPAGE BisTris SDS PAGE gels (Invitrogen) using the X-Cell *SureLock* Mini-Cell electrophoresis system (Invitrogen) and electroblotted onto PVDF membrane (Invitrogen). The membrane was blocked and incubated overnight at 4°C with anti-$p75^{NTR}$ antibody (Millipore). The membrane was then probed with horseradish peroxidase (HRP)-conjugated goat anti-rabbit antibody and visualized with ECL reagents (Immobilon Western, Millipore). The chemiluminescent signal was recorded using the BioSpectrum AC Imaging system (UVP).

Immunohistochemistry

Embryos (E10) were fixed in 4% paraformaldehyde in phosphate-buffered saline (PBS) at 4°C for 1 h, dehydrated, cleared in toluene, and embedded in paraffin. Serial 7-μm-thick transverse sections were mounted on Superfrost Plus slides (Fisher Scientific). After epitope recovery by proteinase K digestion (20 μg ml^{-1} for 6 min at room temperature), sections were incubated with anti-$p75^{NTR}$ rabbit anti-mouse primary antibody (Advanced Targeting Systems) at 1:200 dilution at 4°C overnight followed by Alexa Fluor 488-conjugated goat anti-rabbit IgG (Invitrogen) secondary antibody labeling. Vectashield mounting medium with DAPI for fluorescence (Vector Laboratories) was used for mounting slides and staining nuclei. The results were examined and recorded on an Olympus BX51 microscope and photographed using a DP71 camera and DP controller software (Olympus).

Sciatic Nerve Analysis

Postnatal 1- to 3-month-old control and mutant mice were perfused with 4% paraformaldehyde and the left and right sciatic nerves dissected. Semithin plastic sections were prepared and stained with toluidine blue. Mosaic images of entire cross sections of sciatic nerve from comparable anatomic levels were collected using a microscope with a motorized stage (Axiovert 200M, Zeiss). The diameter of the sciatic nerves were measured and compared between mutant and control mice using the analysis software (Axiovision, Zeiss). The data are displayed as the mean ± SEM of four nerves from each genotype. The data were subjected to a student's *t*-test and a *P*-value <0.05 was considered significant.

ACKNOWLEDGMENTS

The authors thank K. Chiu from the CHLA mouse genome core for technical assistance.

LITERATURE CITED

Barker PA. 2004. p75NTR is positively promiscuous: Novel partners and new insights. Neuron 42:529–533.

Bronfman FC. 2007. Metalloproteases and gamma-secretase: New membrane partners regulating p75 neurotrophin receptor signaling? J Neurochem 103 (Suppl 1):91–100.

Chai Y, Jiang X, Ito Y, Bringas P Jr, Han J, Rowitch DH, Soriano P, McMahon AP, Sucov HM. 2000. Fate of the mammalian cranial neural crest during tooth and mandibular morphogenesis. Development 127: 1671–1679.

Dudas M, Sridurongrit S, Nagy A, Okazaki K, Kaartinen V. 2004. Craniofacial defects in mice lacking BMP type I receptor Alk2 in neural crest cells. Mech Dev 121:173–182.

Harlow E, Lane D. 1988. Antibodies. A laboratory manual. New York: CSH Press.

Holzenberger M, Lenzner C, Leneuve P, Zaoui R, Hamard G, Vaulont S, Bouc YL. 2000. Cre-mediated germline mosaicism: A method allowing rapid generation of several alleles of a target gene. Nucleic Acids Res 28:E92.

Jiang X, Rowitch DH, Soriano P, McMahon AP, Sucov HM. 2000. Fate of the mammalian cardiac neural crest. Development 127:1607–1616.

Kaartinen V, Voncken JW, Shuler C, Warburton D, Bu D, Heisterkamp N, Groffen J. 1995. Abnormal lung development and cleft palate in mice lacking TGF-beta 3 indicates defects of epithelial-mesenchymal interaction. Nat Genet 11:415–421.

Lee KF, Bachman K, Landis S, Jaenisch R. 1994a. Dependence on p75 for innervation of some sympathetic targets. Science 263:1447–1449.

Lee KF, Davies AM, Jaenisch R. 1994b. p75-deficient embryonic dorsal root sensory and neonatal sympathetic neurons display a decreased sensitivity to NGF. Development 120:1027–1033.

Lee KF, Li E, Huber LJ, Landis SC, Sharpe AH, Chao MV, Jaenisch R. 1992. Targeted mutation of the gene encoding the low affinity NGF receptor p75 leads to deficits in the peripheral sensory nervous system. Cell 69:737–749.

Lim YS, McLaughlin T, Sung TC, Santiago A, Lee KF, O'Leary DD. 2008. p75(NTR) mediates ephrin-A reverse signaling required for axon repulsion and mapping. Neuron 59:746–758.

Paul CE, Vereker E, Dickson KM, Barker PA. 2004. A pro-apoptotic fragment of the p75 neurotrophin receptor is expressed in p75NTRExonIV null mice. J Neurosci 24:1917–1923.

Peterson S, Bogenmann E. 2003. Osmotic swelling induces p75 neurotrophin receptor (p75NTR) expression via nitric oxide. J Biol Chem 278:33943–33950.

Roux PP, Barker PA. 2002. Neurotrophin signaling through the p75 neurotrophin receptor. Prog Neurobiol 67:203–233.

Tomita K, Kubo T, Matsuda K, Fujiwara T, Yano K, Winograd JM, Tohyama M, Hosokawa K. 2007. The neurotrophin receptor p75NTR in Schwann cells is implicated in remyelination and motor recovery after peripheral nerve injury. Glia 55:1199–1208.

Underwood CK, Coulson EJ. 2008. The p75 neurotrophin receptor. Int J Biochem Cell Biol 40:1664–1668.

von Schack D, Casademunt E, Schweigreiter R, Meyer M, Bibel M, Dechant G. 2001. Complete ablation of the neurotrophin receptor p75NTR causes defects both in the nervous and the vascular system. Nat Neurosci 4:977–978.

Xu X, Li C, Garrett-Beal L, Larson D, Wynshaw-Boris A, Deng CX. 2001. Direct removal in the mouse of a floxed neo gene from a three-loxP conditional knockout allele by two novel approaches. Genesis 30:1–6.

Yang LT, Kaartinen V. 2007. Tgfb1 expressed in the Tgfb3 locus partially rescues the cleft palate phenotype of Tgfb3 null mutants. Dev Biol 312:384–395.